

Visible absorption bands of the $(\text{O}_2)_2$ collision complex at pressures below 760 Torr

Hans Naus and Wim Ubachs

The collision-induced absorption of oxygen in the 540–650-nm wavelength region has been measured at a pressure range from 0 to 730 Torr at $T = 294$ K. Pressure-dependent cross sections of the $X^3\Sigma_g^+ + X^3\Sigma_g^+ \rightarrow a^1\Delta_g(v=0) + a^1\Delta_g(v=1)$ and $X^3\Sigma_g^+ + X^3\Sigma_g^+ \rightarrow a^1\Delta_g(v=0) + a^1\Delta_g(v=0)$ transitions have been determined by means of cavity-ringdown spectroscopy. Contributions of the overlapping γ and δ bands of O_2 have been evaded, and Rayleigh extinction has been taken into account. © 1999 Optical Society of America

OCIS codes: 020.2070, 290.1310, 300.1030.

1. Introduction

Observations of weak and broad absorption resonances in the oxygen spectrum were reported as early as 1885.¹ Through further detailed studies in the 1930's it was established^{2,3} that these absorption features originate from the oxygen collision complex, and even at that early stage it was understood that both collision partners undergo an electronic transition during the collision process. Subsequently the O_2 complex was studied at lower temperatures,⁴ while some weak absorption phenomena in the 200–280-nm UV range were also observed.⁵ By now the $(\text{O}_2)_2$ absorptions are well characterized, and pressure-dependent cross sections have been derived through the work of Dianov-Klokov,⁶ Greenblatt *et al.*,⁷ and recently Newnham and Ballard.⁸

The collisional complexes relate to an O_2 – O_2 interaction potential, and the broad absorption features observed at room temperature correspond to continuum states at positive energies. In the negative energy region of the electronic ground state of the dimer, with a well depth of some 150 cm^{-1} due to van der Waals interactions,⁹ there exist bound states that were investigated in a liquid- N_2 -cooled cell by Long and Ewing¹⁰ and recently in jet experiments by Cam-

pargue *et al.*¹¹ These $(\text{O}_2)_2$ van der Waals complexes should not be confused with covalently bound O_4 molecules that were observed in an electronically excited state.¹² An important result of previous work is that at room temperature no significant structure exists in the broad collisionally induced absorption bands; these features can be considered as essentially continuous even at the highest resolution.

The oxygen collision complex was first observed in the Earth's atmosphere by Perner and Platt.¹³ The amount of solar radiation absorbed by $(\text{O}_2)_2$ was discussed by Pfeilsticker *et al.*¹⁴ In a recent review Solomon *et al.*¹⁵ have estimated the globally averaged all-sky radiation budget of oxygen complexes, including O_2 – N_2 , at 1 Wm^{-2} . Accurate data on the oxygen complexes may be of practical interest for atmospheric research. Erle *et al.*¹⁶ suggested that the broad ($>300\text{-cm}^{-1}$) absorptions of $(\text{O}_2)_2$ may be used to determine the path length of photons through clouds. Since water-vapor absorptions of $\sim 580 \text{ nm}$ are minimal, the yellow band of the oxygen complex, which has the largest intensity, is likely to be most suitable for such a purpose.

In this paper we report on a laboratory reexamination of the 580- and the 630-nm collisionally induced oxygen bands with the laser-based technique of cavity-ringdown spectroscopy (CRDS). These absorption bands can be assigned as $X^3\Sigma_g^+ + X^3\Sigma_g^+ \rightarrow a^1\Delta_g + a^1\Delta_g(v=1)$ and $X^3\Sigma_g^+ + X^3\Sigma_g^+ \rightarrow a^1\Delta_g + a^1\Delta_g$. Here and below $X^3\Sigma_g^+(v=0)$ and $a^1\Delta_g(v=0)$ are assumed if the vibrational assignment is not specified. The sensitivity of our CRDS setup enabled us to examine the collisionally induced absorption of oxygen throughout the entire atmospheric-relevant pressure range of 0–730 Torr at room

The authors are with the Department of Physics and Astronomy, Vrije Universiteit, De Boelelaan 1081, 1081 HV Amsterdam, The Netherlands. The e-mail address for H. Naus is naus@nat.vu.nl. The e-mail address for W. Ubachs is wimu@nat.vu.nl.

Received 26 October 1998; revised manuscript received 4 January 1999.

0003-6935/99/153423-06\$15.00/0

© 1999 Optical Society of America

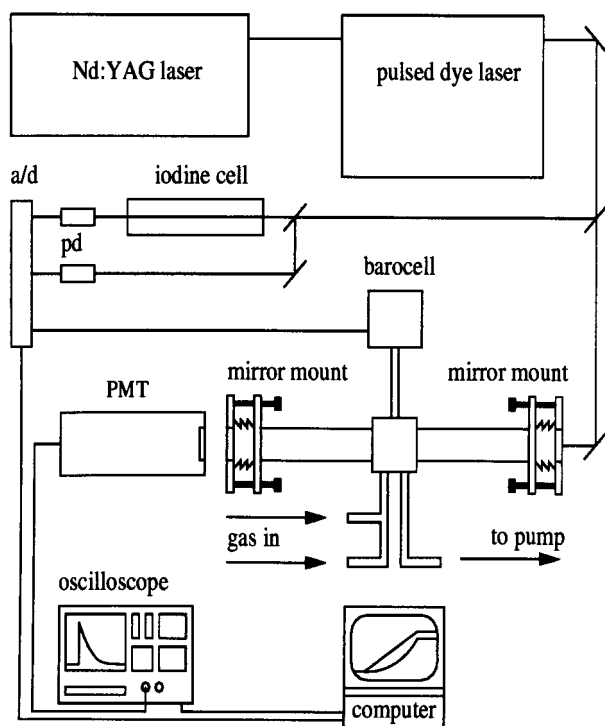


Fig. 1. Schematic display of the experimental setup: a/d, analog-to-digital converter; pd, photodiode; PMT, photomultiplier tube.

temperature. Until now, measurements were done at pressures of 760 Torr (Ref. 8) or higher.^{6,7} By taking discrete steps on the frequency scale, the collisionally induced absorption was unraveled from the absorption of the γ and the δ bands¹⁷ of the oxygen monomer. Moreover, the problem of Rayleigh scattering at low pressures, giving rise to observable extinction at a similar rate as for the oxygen complex, was addressed.

2. Experimental Setup

The experimental setup used in this experiment, schematically shown in Fig. 1, is a typical CRDS setup.¹⁸ It is similar to the one used for studies of the near-infrared oxygen monomer bands of O_2 isotopomers.¹⁹ Tunable pulsed-laser radiation from a Nd:YAG pumped dye laser system (Quanta-Ray PDL-3) running on various dyes is used to cover the frequency range from 15 300 to 18 400 cm^{-1} with a bandwidth of $<0.05 cm^{-1}$.

The laser pulse is coupled into a stable nonconfocal cavity, consisting of two highly reflecting ($R > 99\%$) curved mirrors. After each round trip a small part ($1 - R$) of the trapped light is coupled out at a mirror, while the remaining part is reflected. The intensity of the light leaking from the cavity will decay exponentially in time:

$$I(t) = I_{(t=0)} \exp\left[-\left(\frac{c}{d}\right) |\ln(R)| t\right], \quad (1)$$

where c is the speed of light, d is the cavity length, and R is the reflectivity of the mirrors. The decay rate of an empty cavity β_0 , or empty cavity loss, is the background signal of CRDS:

$$\beta_0 = \frac{c|\ln(R)|}{d}. \quad (2)$$

It is determined by the reflectivity of the mirrors and the cavity length.

Additional losses in the cavity will result in a faster decay of the intensity. If this extra loss satisfies Beer's law, the decay will remain exponential:

$$I(t) = I_{(t=0)} \exp\left\{-\left(\frac{c}{d}\right) [|\ln(R)| + \kappa l] t\right\}, \quad (3)$$

where κ is the extra loss due to extinction by a medium inside the cavity and l is the medium length. The decay rate β , or total cavity loss, will be larger than β_0 :

$$\beta = \frac{c}{d} [|\ln(R)| + \kappa l]. \quad (4)$$

Hence, if $d = l$,

$$\kappa = \frac{(\beta - \beta_0)}{c}. \quad (5)$$

The decay transients were detected with a photomultiplier tube (Thorn EMI 9658 RA), stored on a digital oscilloscope (LeCroy 9450), and on-line fitted to an exponential function by a computer (Sun workstation). The obtained decay rates β , measured as functions of wavelength, constitute an absorption spectrum, in which β_0 forms a background level that may depend on wavelength.

To select a frequency that does not coincide with an O_2 absorption feature, the laser was scanned over a few wave numbers to record an I_2 absorption spectrum. This spectrum was calibrated against the I_2 reference standard.²⁰ The frequency at the end of the scan can thus be determined. The $(O_2)_2$ absorption measurement is performed at that frequency. Afterwards the laser is scanned further to check for possible drifts in the frequency position. The calibration was performed at every position, resulting in an accuracy of better than $0.1 cm^{-1}$.

Two mirror sets were used, one set for the region 15 300–16 600 cm^{-1} (Newport SuperMirrors, $R_{max} = 99.983\%$) and a set for the region 16 850–18 400 cm^{-1} (Research Electro Optics, $R_{max} = 99.997\%$). The noise-equivalent detection limit is $10^{-8} cm^{-1}$ for the red range ($>600 nm$) and $10^{-9} cm^{-1}$ for the yellow range ($<600 nm$) after a summation of five decay transients to reduce the shot noise.

The oxygen pressure in a 86.5-cm-long CRDS cell was gradually increased from 0 to 730 Torr by means of a needle-valve tap. The pressure was simultaneously recorded with the decay transients by means of a capacitance manometer (Edwards 600 AB, 1000 Torr) connected to an analog-to-digital converter.

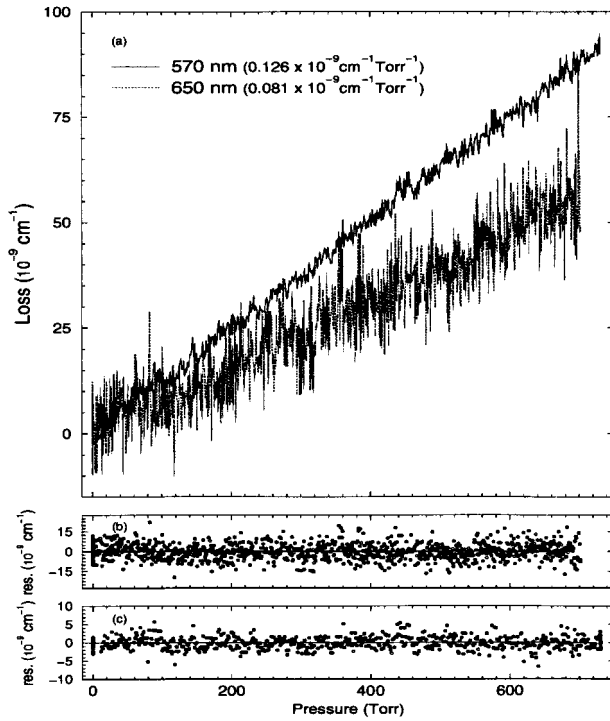


Fig. 2. (a) N_2 extinction versus pressure at 570 and 650 nm (β_0 subtracted), (b) the unweighted residue at 650 nm ($\sigma = 6.3 \times 10^{-9} \text{ cm}^{-1}$), (c) the unweighted residue at 570 nm ($\sigma = 1.8 \times 10^{-9} \text{ cm}^{-1}$).

The pressure change in the cell during a measurement cycle of 0.5 s is comparable with the uncertainty of the recorded pressure (0.1 Torr or 0.15% of the reading) while the increase of the loss rate is negligible. Commercial gas samples [oxygen (2.5) and nitrogen (5.0)] were used without further purification.

The assumption that the decay remains exponential in the case of extra losses is valid only if the bandwidth of the laser pulse is much smaller than the width of the absorption resonance. If this is not true the derived absorption strengths will be systematically underestimated.^{21,22} Because of the broad ($\Delta_{\text{abs}}/\Delta_{\text{laser}} = 6000$) and structureless absorption bands of $(O_2)_2$ the decay will remain exponential and the determined absorption strengths will represent the true values.

3. Data Analyses and Results

At pressures below 760 Torr, Rayleigh scattering gives rise to losses at a rate comparable with absorption by the oxygen complex. To address this issue the extinction due to Rayleigh scattering by N_2 was measured at eight calibrated positions between 570 and 650 nm. Figure 2 shows the measured loss as a function of the pressure at two wavelengths. These pressure-dependent loss curves typically consist of 900 data points. The residues of the unweighted linear fit (Fig. 2) show that the extinction is indeed linear and give an impression of the achieved sensitivity. The larger noise in the data at 650 nm is due to the lower reflectivity of the mirrors. At each of

the eight frequencies a Rayleigh extinction rate is determined.

Rayleigh extinction is, to a good approximation, linear with pressure,^{23,24} so only a linear pressure dependence of the loss κ is expected. The total Rayleigh scattering cross section per molecule $\sigma(\bar{\nu})$ (in square centimeters per molecule) is given by²³

$$\sigma(\bar{\nu}) = \frac{24\pi^3 \bar{\nu}^4 (n_s^2 - 1)^2}{N_s^2 (n_s^2 + 2)^2} \left(\frac{6 + 3\rho_s}{6 - 7\rho_s} \right), \quad (6)$$

where $\bar{\nu}$ is the frequency (in inverse centimeters), n_s is the refractive index at $\bar{\nu}$, N_s is the molecular number density ($2.496 \times 10^{19} \text{ cm}^{-3}$ at $T = 294 \text{ K}$), and ρ_s is the depolarization ratio. With the approximations that the refractive index [$n_{590\text{nm},273.15\text{K}} = 1.000279$ (Ref. 24)] and depolarization [$\rho_{633\text{nm}} = 0.01018$ (Ref. 25)] are constant over the 80-nm wavelength range,²³ while $(n_s - 1)$ is assumed linear with temperature,²⁴ the loss rate $\kappa_{N_2,294\text{K}}$ for N_2 is

$$\kappa_{N_2,294\text{K}}(\bar{\nu}) = 1.35 \times 10^{-27} \bar{\nu}^4 (\text{cm}^{-1} \text{ Torr}^{-1}) \quad (7)$$

with the frequency $\bar{\nu}$ in inverse centimeters. A $\bar{\nu}^4$ fit through the eight measured extinction rates gives

$$\kappa_{\text{exp}}(\bar{\nu}) = 1.36(0.02) \times 10^{-27} \bar{\nu}^4 (\text{cm}^{-1} \text{ Torr}^{-1}) \quad (8)$$

with the estimated error (1σ) in parentheses.

The clearly visible linear pressure dependence of the loss κ (Fig. 2) indeed shows that Rayleigh extinction cannot be neglected at the sensitivity level of the present measurements. Since the Rayleigh cross sections for N_2 and O_2 are comparable, the linear Rayleigh contribution to the measured loss $\kappa_{O_2}(P)$ should be accounted for. Because two, and only two, O_2 molecules are involved in the collision-induced absorption process the absorption due to oxygen will be quadratic in pressure.^{3,4} Hence the loss for the measurements on oxygen as a function of the pressure should be a second-order polynomial:

$$\kappa_{O_2}(P) = \beta_0 + \kappa_{\text{lin}} P + \kappa_{\text{sq}} P^2, \quad (9)$$

where β_0 is the empty cavity loss. Figure 3 shows three loss curves of O_2 measured at three different frequency positions. A nonlinear behavior is clearly visible in curves I and II, but curve III also contains a nonlinear term. The insets show the weighted residues of a second-order polynomial fit. All three curves are well described by Eq. (9). A pressure-dependent extinction curve was measured for over 200 frequencies in the range 15 300–18 400 cm^{-1} . A three-parameter fit to the measured curves results in three frequency-dependent loss terms: β_0 , a linear extinction coefficient κ_{lin} due to the Rayleigh extinction, and the quadratic absorption coefficient κ_{sq} .

The linear extinction coefficients κ_{lin} of the $(O_2)_2$ absorption curves represent the Rayleigh extinction and should thus have a $\bar{\nu}^4$ dependence. The $\bar{\nu}^4$ function fitted to these linear extinction coefficients results in a functional form:

$$\kappa_{\text{lin},O_2}(\bar{\nu}) = 1.25(0.02) \times 10^{-27} \bar{\nu}^4 (\text{cm}^{-1} \text{ Torr}^{-1}). \quad (10)$$

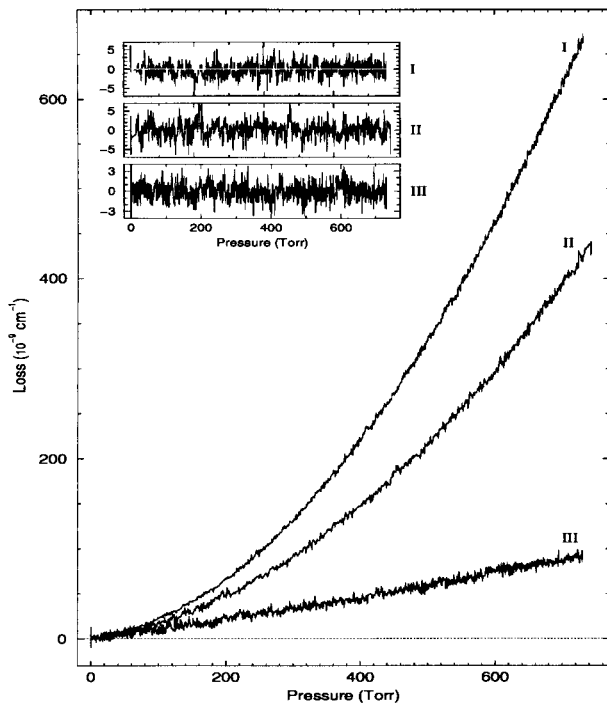


Fig. 3. O_2 loss curves (β_0 subtracted) at three different frequencies (I, 17401.1 cm^{-1} ; II, 17206.1 cm^{-1} ; III, 16887.7 cm^{-1}). The insets show the weighted residues of a second-order polynomial fit.

According to Eq. (6) the extinction $\kappa_{O_2,294K}(\bar{\nu})$ for oxygen [$n_{590nm,273.15K} = 1.0002715$ (Ref. 24), $\rho_{633nm} = 0.0302$ (Ref. 25)] is

$$\kappa_{O_2,294K}(\bar{\nu}) = 1.20 \times 10^{-27} \bar{\nu}^4 (\text{cm}^{-1} \text{ Torr}^{-1}). \quad (11)$$

The linear extinction term as determined from the measurements is well represented by a $\bar{\nu}^4$ dependence, as expected for Rayleigh scattering, and it also agrees reasonably well with the expected extinction according to Eq. (11). The agreement between the measured and the calculated Rayleigh extinction of N_2 is better because only a linear pressure dependence of the loss rate at a certain frequency is present. Another source of uncertainty, in the case of oxygen, is the substantial spread in values for the depolarization ratios reported in the literature.²⁶

Subsequently the linear coefficient κ_{lin} in Eq. (9) is equated to the expected value obtained from the present experimental data, Eq. (10), and implemented in a two-parameter fit (β_0, κ_{sq}) for a reanalysis of the data. This results in reduced noise for the quadratic coefficient because the correlation between the quadratic and the linear terms disappears. Particularly in the wings of the $(O_2)_2$ absorption curves the resulting values for the linear and the quadratic coefficients κ_{lin} and κ_{sq} were strongly correlated in the three-parameter fit. Here the uncertainty and the spread in the values for κ_{sq} are largely reduced. In Fig. 4 this is shown for the frequency range $18\,000\text{--}18\,400\text{ cm}^{-1}$, corresponding to the blue wing of the $\Delta\nu = 1$ resonance.

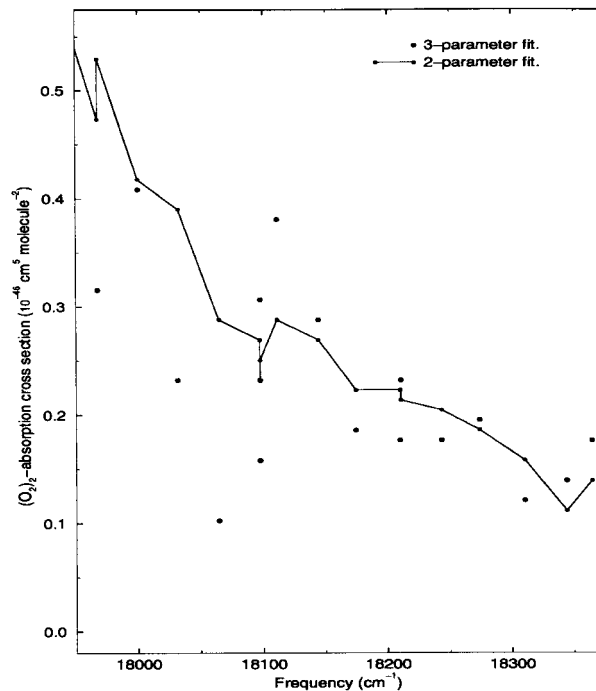


Fig. 4. Uncertainty in the quadratic coefficient κ_{sq} is largely reduced in the far wing of the absorption if the linear coefficient is kept fixed at the estimated value from Eq. (10).

The I_2 frequency calibration and the narrow laser bandwidth made it possible to omit frequencies coinciding with an absorption of the γ or the δ band of O_2 . Effects of absorption due to these O_2 bands are absent in our measurements. A margin of a few wave numbers between an O_2 absorption and the actual position is necessary because the absorption in the wing of a resonance will not be linear with the pressure (because of pressure broadening and laser bandwidth effects) and would thus contribute to the nonlinear behavior of the total loss.

To check the reproducibility of the data, measurements at one frequency ($17\,315.1\text{ cm}^{-1}$) were done on different days. Six measurements give an average absorption cross section of $11.40 \times 10^{-46}\text{ cm}^5\text{ molecule}^{-2}$ with a standard deviation of 0.65%.

The final results of the data analyses are shown in Fig. 5. Here the resulting values of κ_{sq} , pertaining to the effect of collision-induced absorption, are plotted as functions of wavelength. The two absorption bands are fitted to skewed Voigt profiles. These profiles have no physical meaning, but a function format enables easier determination of relevant band parameters (Tables 1 and 2) and comparison with existing data.^{7,8}

The noise near $16\,400\text{ cm}^{-1}$ is due to the lower reflectivity ($<99.97\%$) of the mirrors at these frequencies and the small absorption coefficient κ_{sq} . At frequencies $>18\,000\text{ cm}^{-1}$ the fitted line profile slightly deviates from the data. This small deviation may be attributed to the far wing of another weak collision-induced absorption resonance at $18\,800\text{ cm}^{-1}$,^{7,8} which is not included in the present analyses. The

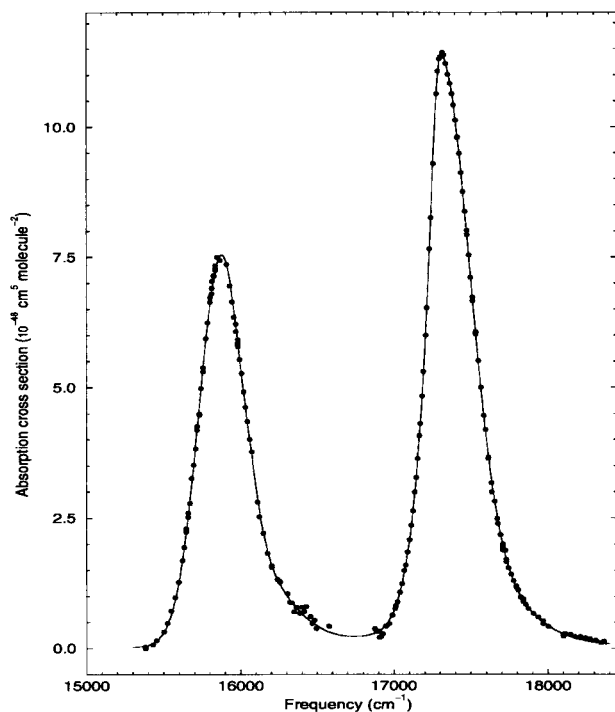


Fig. 5. $(\text{O}_2)_2$ collision-induced absorption cross section. The solid curve represents the skewed Voigt profiles fitted to the data.

most recent data^{7,8} and the data of this work are shown in Fig. 6. The original data of Newnham and Ballard⁸ are also fitted to skewed Voigt profiles for better comparison.

The absorption cross section for the $(\text{O}_2)_2$ collision complex as determined by Newnham and Ballard is zero to the left and the right of each absorption band. This may be explained by the fact that Newnham and Ballard used an empty cell spectrum to determine the background and corrected the transmittance to 1 at nonabsorbing points.⁸ Hence the background was

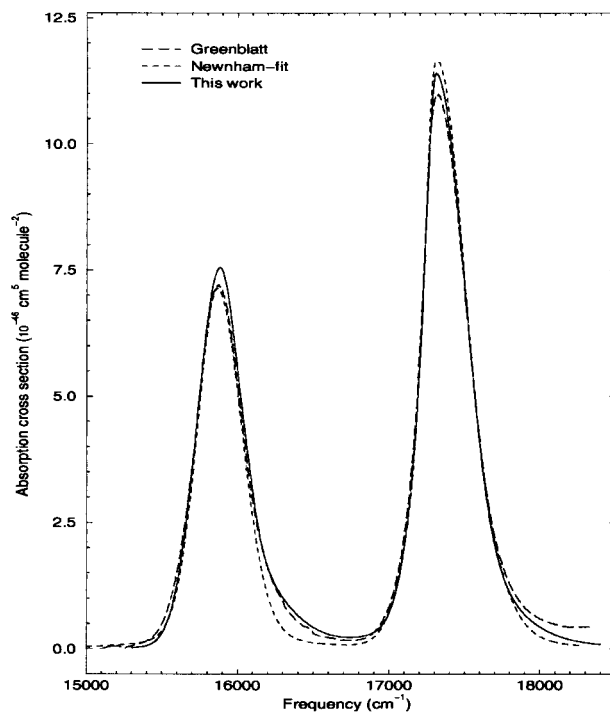


Fig. 6. Absorption cross sections of $(\text{O}_2)_2$ from the works of Greenblatt *et al.*⁷ and Newnham and Ballard⁸ and this work. The data of Ref. 8 are fitted to a functional form for better comparison (see text).

explicitly set to zero. Greenblatt *et al.*⁷ performed their experiments at much higher pressures and used a cell pressurized with nitrogen at 90% of the oxygen pressure to record a background spectrum.

The band parameters of the $(\text{O}_2)_2$ absorption bands as determined in this experiment are in good agreement with the studies of Greenblatt *et al.*⁷ and Newnham and Ballard⁸; see Tables 1 and 2. The only deviation is the band intensity of the $X^3\Sigma_g^+ + X^3\Sigma_g^+$

Table 1. Band Parameters of the $X^3\Sigma_g^+ + X^3\Sigma_g^+ \rightarrow a^1\Delta_g + a^1\Delta_g$ Resonance^a

Parameter	Greenblatt <i>et al.</i> ⁷	Newnham and Ballard ⁸	This Work
Position (cm^{-1})	15 869 (5)	15 862 (5)	15 880 (1)
Width (cm^{-1})	368 (5)	369 (5)	367 (1)
Peak absorption ($10^{-46} \text{ cm}^5 \text{ molecule}^{-2}$)	7.2 (2)	7.1 (2)	7.55 (5)
Band intensity ($10^{-43} \text{ cm}^4 \text{ molecule}^{-2}$)	3.1 (1)	2.8 (1)	3.19 (3)

^aThe position is defined as the maximum of the absorption, and the width is defined as the bandwidth at half the band absorbance. The numbers in parentheses are the 1σ uncertainty in the last digit.

Table 2. Band Parameters of the $X^3\Sigma_g^+ + X^3\Sigma_g^+ \rightarrow a^1\Delta_g + a^1\Delta_g(\nu = 1)$ Resonance^a

Parameter	Greenblatt <i>et al.</i> ⁷	Newnham and Ballard ⁸	This Work
Position (cm^{-1})	17 320 (5)	17 314 (5)	17 308 (1)
Width (cm^{-1})	348 (5)	339 (5)	340 (1)
Peak absorption ($10^{-46} \text{ cm}^5 \text{ molecule}^{-2}$)	11.0 (3)	11.7 (3)	11.41 (5)
Band intensity ($10^{-43} \text{ cm}^4 \text{ molecule}^{-2}$)	4.8 (1)	4.7 (1)	4.66 (3)

^aThe position is defined as the maximum of the absorption, and the width is defined as the bandwidth at half the band absorbance. The numbers in parentheses are the 1σ uncertainty in the last digit.

$\rightarrow a \ ^1\Delta_g + a \ ^1\Delta_g$ absorption band of the measurements of Newnham and Ballard. This may be caused by the fact that Newnham and Ballard had to correct their data for the background and the absorption because of the γ band of the oxygen monomer. Greenblatt *et al.* performed their measurements at high pressures, up to 55 atm, at which the relative effect of the absorption due to the γ band is negligible. In our data we totally evaded the effect of this contribution by choosing discrete measurement positions in between the monomer resonances in combination with a narrow-band light source.

4. Conclusions

By means of CRDS the band parameters of the $X \ ^3\Sigma_g^+ + X \ ^3\Sigma_g^+ \rightarrow a \ ^1\Delta_g + a \ ^1\Delta_g (v = 1)$ and $X \ ^3\Sigma_g^+ + X \ ^3\Sigma_g^+ \rightarrow a \ ^1\Delta_g + a \ ^1\Delta_g$ transitions have been determined from measurements in a pressure range from 0 to 730 Torr. Contributions of the overlapping γ and δ bands of O_2 have been evaded, and Rayleigh extinction has been taken into account. The accuracy of the band parameters is improved. It is confirmed that the collision-induced absorption of oxygen is a quadratic function of the pressure throughout the entire pressure range for all wavelengths. The determined Rayleigh extinction rates are in good agreement with the expected values, verifying our data analyses.

The authors thank S. Solomon and J. B. Burkholder for helpful discussions and D. A. Newnham for making data available before publication. The Space Research Organization Netherlands is acknowledged for financial support.

References

- J. Janssen, "Analyse spectrale des éléments de l'atmosphère terrestre," *C. R. Acad. Sci.* **101**, 649–651 (1885).
- J. W. Ellis and H. O. Kneser, "Kombinationsbeziehungen im Absorptionsspektrum des flüssigen Sauerstoffes," *Z. Phys.* **86**, 583–591 (1933).
- H. Salow and W. Steiner, "Die durch Wechselwirkungskräfte bedingten Absorptionsspektren des Sauerstoffes, I. Die Absorptionsbanden des (O_2-O_2) -Moleküls," *Z. Phys.* **99**, 137–158 (1936).
- R. P. Blickensderfer and G. E. Ewing, "Collision-induced absorption spectrum of gaseous oxygen at low temperatures and pressures. II. The simultaneous transitions $^3\Sigma_g^+ + ^3\Sigma_g^+ \rightarrow ^1\Delta_g + ^1\Delta_g$ and $^3\Sigma_g^+ + ^3\Sigma_g^+ \rightarrow ^1\Delta_g + ^1\Sigma_g^+$," *J. Chem. Phys.* **51**, 5284–5289 (1969).
- Shardanand, "Absorption cross sections of O_2 and O_4 between 2000 and 2800 Å," *Phys. Rev.* **186**, 5–9 (1969).
- V. I. Dianov-Klokov, "Absorption spectrum of oxygen at pressures from 2 to 35 atm. in the region 12,600 to 3600 Å," *Opt. Spectrosc.* **16**, 224–227 (1964).
- G. D. Greenblatt, J. J. Orlando, J. B. Burkholder, and A. R. Ravishankara, "Absorption measurements of oxygen between 330 and 1140 nm," *J. Geophys. Res.* **95**, 18577–18582 (1990).
- D. A. Newnham and J. Ballard, "Visible absorption cross-sections and integrated absorption intensities of molecular oxygen (O_2 and O_4)," *J. Geophys. Res.* **103**, 28801–28816 (1998).
- P. E. S. Wormer and A. van der Avoird, "(Heisenberg)exchange and electrostatic interactions between O_2 molecules: An *ab initio* study," *J. Chem. Phys.* **81**, 1929–1940 (1984).
- C. A. Long and G. E. Ewing, "Spectroscopic investigation of van der Waals molecules. I. The infrared and visible spectra of $(O_2)_2$," *J. Chem. Phys.* **58**, 4824–4834 (1973).
- A. Campargue, L. Biennier, A. Kachanov, R. Jost, B. Bussery-Honvault, V. Veyret, S. Churassy, and R. Bacis, "Rotationally resolved absorption spectrum of the O_2 dimer in the visible range," *Chem. Phys. Lett.* **288**, 734–742 (1998).
- H. M. Bevssek, M. Ahmed, D. S. Peterka, F. C. Sailes, and A. G. Suits, "Direct detection and spectroscopy of O_4 ," *Faraday Discuss. Chem. Soc.* **108**, 131–138 (1997).
- D. Perner and U. Platt, "Absorption of light in the atmosphere by collision pairs of oxygen $(O_2)_2$," *Geophys. Res. Lett.* **7**, 1053–1056 (1980).
- K. Pfeilsticker, F. Erle, and U. Platt, "Absorption of solar radiation by atmospheric O_4 ," *J. Atmos. Sci.* **54**, 933–939 (1997).
- S. Solomon, R. W. Portmann, R. W. Sanders, and J. S. Daniel, "Absorption of solar radiation by water vapor, oxygen, and related collision pairs in the Earth's atmosphere," *J. Geophys. Res.* **104**, 3847–3858 (1998).
- F. Erle, K. Pfeilsticker, and U. Platt, "On the influence of tropospheric clouds on zenith-scattered-light measurements of stratospheric species," *Geophys. Res. Lett.* **22**, 2725–2728 (1995).
- H. B. Babcock and L. Herzberg, "Fine structure of the red system of atmospheric oxygen bands," *Astrophys. J.* **108**, 167–190 (1948).
- M. D. Wheeler, S. M. Newman, A. J. Orr-Ewing, and M. N. R. Ashfold, "Cavity ring-down spectroscopy," *J. Chem. Soc. Faraday Trans.* **94**, 337–351 (1998).
- H. Naus, A. de Lange, and W. Ubachs, " $b \ ^1\Sigma_g^+ - X \ ^3\Sigma_g^+ (0,0)$ band of oxygen isotopomers in relation to tests of the symmetrization postulate in $^{16}O_2$," *Phys. Rev. A* **56**, 4755–4763 (1997).
- S. Gerstenkorn and P. Luc, *Atlas du Spectre d'Absorption de la Molecule de l'Iode entre 14800–20000 cm^{-1}* (Centre National de la Recherche Scientifique, Paris, 1978).
- P. Zalicki and R. N. Zare, "Cavity ring-down spectroscopy for quantitative absorption measurements," *J. Chem. Phys.* **102**, 2708–2717 (1995).
- R. T. Jongma, M. G. H. Boogaarts, I. Holleman, and G. Meijer, "Trace gas detection with cavity-ring-down-spectroscopy," *Rev. Sci. Instrum.* **66**, 2821–2828 (1995).
- A. Bucholtz, "Rayleigh-scattering calculations for the terrestrial atmosphere," *Appl. Opt.* **34**, 2765–2773 (1995).
- R. C. Weast, ed., *Handbook of Chemistry and Physics*, 62nd ed. (CRC, Boca Raton, Fla., 1981–1982), p. E-381.
- N. J. Bridge and A. D. Buckingham, "The polarization of laser light scattered by gases," *Proc. R. Soc. (London) A* **295**, 334–349 (1966).
- A. T. Young, "Revised depolarization corrections for atmospheric extinction," *Appl. Opt.* **19**, 3427–3428 (1980).